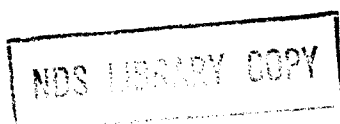


NEANDC (E) 200 "L"  
INDC (FR) 31/L

**COHERENT OPTICAL AND STATISTICAL MODEL CALCULATIONS  
OF NEUTRON CAPTURE CROSS SECTIONS FOR SAMARIUM  
ISOTOPES BETWEEN 1 keV AND 3 MeV**

*J.P. DELAROCHE, Ch. LAGRANGE*



Service de Physique Neutronique et Nucléaire  
Centre d'Etudes de Bruyères-le-Châtel  
B.P. N° 561  
92542 MONTROUGE CEDEX France

JUIN 1980

COMMISSARIAT A L'ENERGIE ATOMIQUE  
FRANCE



NEANDC (E) 200 "L"  
INDC (FR) 31/L

COHERENT OPTICAL AND STATISTICAL MODEL CALCULATIONS  
OF NEUTRON CAPTURE CROSS SECTIONS FOR SAMARIUM  
ISOTOPES BETWEEN 1 keV AND 3 MeV<sup>\*</sup>

J.P. DELAROCHE, Ch. LAGRANGE

*Service de Physique Neutronique et Nucléaire - Centre d'Etudes de Bruyères-le-Châtel  
B.P. n° 561 - 92542 MONTROUGE - France -*

\* Work presented as a Contributed Paper at the "Second Advisory Group Meeting  
on Fission Product Nuclear Data" - Petten, Netherlands, 5-9 September 1977.

JUIN 1980

COMMISSARIAT A L'ENERGIE ATOMIQUE  
FRANCE



Jean-Paul DELAROCHE, Christian LAGRANGE

COHERENT OPTICAL AND STATISTICAL MODEL CALCULATIONS  
OF NEUTRON CAPTURE CROSS SECTIONS FOR SAMARIUM  
ISOTOPES BETWEEN 1 keV AND 3 MeV

J.P. DELAROCHE, Ch. LAGRANGE

*Service de Physique Neutronique et Nucléaire*

*Centre d'Etudes de Bruyères-le-Châtel*

*B.P. N° 561*

*92542 MONTROUGE CEDEX, France*

ABSTRACT -

We show that neutron transmission coefficients, obtained from adapted optical potentials, may be used with success, even in the keV region, in statistical model calculations. Illustrations are given for  $^{147,148,149,150,151,152}$ ,  $^{154}$ Sm capture cross sections below 3 MeV.

CALCULS COHERENTS PAR MODELES OPTIQUE ET STATISTIQUE

DES SECTION EFFICACES DE CAPTURE NEUTRONIQUE POUR

DES ISOTOPES DU SAMARIUM ENTRE 1 keV ET 3 MeV

RESUME -

Nous montrons que des coefficients de transmission de neutrons, obtenus à partir de potentiels optiques adaptés, peuvent être utilisés avec succès, même dans la région du keV, dans des calculs de modèle statistique. Des illustrations sont données pour les sections efficaces de capture neutronique par  $^{147,148,149,150,151,152,154}$ Sm en dessous de 3 MeV.

I - INTRODUCTION -

Since its origin, the statistical model has been extensively used for the interpretation of neutron cross sections, such as capture  $\sigma(n,\gamma)$  and inelastic  $\sigma(n,n')$  at low energy (1 keV - 5 MeV). Its uncertain success was (and remains) strongly dependent on the strength and the energy variations of the neutron transmission coefficients ( $T_c$ ). These coefficients may in principle be obtained from the optical potential determined from an analysis of neutron scattering data (such as angular distributions). However, such analyses are mostly made at one or a few energies in the MeV region. As a consequence, the optical potential parameters so determined may be good enough within a narrow energy range, but cannot easily be extrapolated towards the low energy region. Below 100 keV where the neutron capture cross sections are very sensitive to changes in transmission coefficients, the optical model is generally assumed inadequate and the "strength function model" is mostly used for capture cross section calculations [1].

Such difficulties may be avoided if one uses a method that leads to the determination of optical potentials giving good agreement between experimental and calculated s- and p-wave strength functions  $S_0$  and  $S_1$ , potential scattering radius  $R'$  and total cross sections from a few keV to 20 MeV (and more).

If such a method is used for each target nucleus, it is easy to determine the coefficients  $T_c$  from 1 keV to 3 MeV (for example) and thus to perform statistical model calculations for  $\sigma(n,\gamma)$ . Some calculations and comparisons to experimental capture cross sections of  $^{147,148,149,150,152}$ ,  $^{154}\text{Sm}$  are shown as illustrations of the above coherent procedure. The capture cross section is also given for the unstable target nucleus  $^{151}\text{Sm}$ .

## II - OPTICAL MODEL POTENTIAL -

Following the so-called SPRT-method [2], the optical potential is determined when it leads simultaneously to good fits on  $S_0$ ,  $S_1$ ,  $R'$  and on the energy variations of the total cross section  $\sigma_T$ . This cross section is of some importance because it is the only cross section for which the energy averaged measurement is directly comparable to optical model calculations over the full energy range. This method has been successfully used to determine the neutron optical potential of some nuclei, such as  $^{93}\text{Nb}$  [3] and  $^{148,150,152,154}\text{Sm}$  [4,5].

The optical potential  $U$  has the standard following form :

$$U = - V_R f(r, \alpha_R, R_R) + 4 i \alpha_D W_D \frac{d}{dr} f(r, \alpha_D, R_D) \\ + 2 V_{SO} \frac{\chi^2}{\pi} \frac{1}{r} \frac{d}{dr} f(r, \alpha_{SO}, R_{SO}) \vec{\ell} \cdot \vec{s}. \quad (1)$$

in which  $f(r, \alpha_i, R_i)$  is the Woods-Saxon form factor ;  $R_i = \bar{R}_i \left[ 1 + \beta_2 Y_2^0(\theta') \right]$  for rotational nuclei ;  $R_i = \bar{R}_i \left[ 1 + \beta_2 Y_2^0(\theta) \right]$  for vibrational nuclei ; and  $\bar{R}_i = r_i A^{1/3}$ . An improved version of the JUPITOR-1 code is used [6].

A vibrational model is assumed for  $^{148}\text{Sm}$  and a rotational model for  $^{152,154}\text{Sm}$ . The collective nature of excited states in  $^{150}\text{Sm}$  is more complex. For this transitional nucleus either a rotational model or a vibrational model can be assumed.

In the present work, no optical model calculations have been performed for the odd samarium isotopes. The assumptions that we have done for them are explained later along with the statistical model calculations.

The optical potential parameters used in this work are essentially those which were published previously [4,5]. The main difference consists in the energy variation of  $W_D$  which has been changed so as to match the experimental elastic and inelastic scattering angular distributions at 4.1 MeV [5]. This new parameterization which will be published elsewhere does not change the accuracy of the fits previously published.

In Tables 1 and 2 are shown the calculated and measured [7-16] strength functions  $S_0$  and  $S_1$  for the even isotopes.

### III - STATISTICAL MODEL CALCULATIONS -

In the following statistical model calculations the only de-excitation modes available to the compound nuclei in the mass region and energy range considered are elastic and inelastic scattering and capture. The transmission coefficients  $T_c$  values are chosen identical for all the open channels and assumed equal to the ground state channels ones. These hypotheses, though not well justified, are widely assumed in statistical model calculations.

The transmission coefficients  $T_c$  for even isotopes are determined from coupled channel calculations. As for the odd isotopes  $^{149,151}\text{Sm}$  it has been assumed that  $T_c$  values can be obtained by averaging the  $T_c$  coefficients associated to the neighbouring even isotopes as follows :

$$T_c(^{149}\text{Sm}) = \frac{1}{2} \left[ T_c(^{148}\text{Sm}) + T_c(^{150}\text{Sm}) \right] \quad (2)$$

and

$$T_c(^{151}\text{Sm}) = \frac{1}{2} \left[ T_c(^{150}\text{Sm}) + T_c(^{152}\text{Sm}) \right].$$

The  $T_c(^{150}\text{Sm})$  have been determined as :

$$T_c(^{150}\text{Sm}) \equiv \frac{1}{2} \left[ T_c(^{150}\text{Sm; vibr.}) + T_c(^{150}\text{Sm; rot.}) \right], \quad (3)$$

where the notation vibr. (resp. rot.) means that vibrational (resp. rotational) model is assumed. As for the transmission coefficients  $T_c(^{147}\text{Sm})$  we have made the following assumption :

$$T_c(^{147}\text{Sm}) \equiv T_c(^{148}\text{Sm}), \quad (4)$$

These transmission coefficients can be used to compute the strength functions  $S_0$  and  $S_1$  for  $^{147,149,151}\text{Sm}$ . The results of calculations and measurements [7-16] of  $S_0$  and  $S_1$  for these isotopes are compared in the Tables 1 and 2.

The compound nucleus cross section for all open channels  $cc'$  with total angular momentum and parity  $J\Pi$  may be written [17] :

$$\sigma_{(cc')}^{J\Pi} = \pi \chi_c^2 \left[ \langle \frac{\theta_c \theta_{c'}}{\theta} \rangle^{J\Pi} - \frac{\delta_{cc'}}{4} Q_c^{J\Pi} \langle \theta_c \rangle^{J\Pi} \right] \quad (5)$$

For neutron channels, the  $\theta_c$  coefficients are identified to the above  $T_c$  coefficients if  $Q_c^{J\Pi} = 0$ . At neutron energy  $E_n$ , the transmission coefficients  $T_\gamma^{J\Pi}(E_n)$  for channel  $\gamma$  may be expressed as  $T_\gamma^{J\Pi}(E_n) = 2 \pi \rho_{CN}^{J\Pi}(E) \Gamma_\gamma^{J\Pi}(E)$  in which  $\rho_{CN}^{J\Pi}(E)$  is the level density at excitation energy  $E$  of the compound nucleus.

- In the present calculations, the following approximations are made :
- . If  $E \geq E_x$ , the Gilbert and Cameron formula [18] is assumed for  $\rho_{CN}^{J\Pi}$  which depends on the level density parameter "a" and the spin cut-off  $\sigma$ . An estimate for  $\sigma^2$  is given by the formula :  $\sigma^2(E) = 0.0888\sqrt{a} E^{2/3}$  [18].
  - . If  $E \leq E_x$ , the  $J\Pi$  independent part  $\rho_{CN}^{J\Pi}(E)$  of  $\rho_{CN}^{J\Pi}(E)$  has an exponential energy variation :  $\rho_{CN}^{J\Pi}(E) = \frac{1}{T} \exp[(E-E_0)/T]$ . The parameters  $E_x$ ,  $E_0$  and  $T$  are then adjusted to known low-lying excited states of the compound nucleus, ( $CN$ ) and  $\sigma^2(E) = \sigma^2(E_x)$ .
  - . The target level density  $\rho_T^{I\Pi}(E)$  contains a discrete part (the excited states with known and assumed spins and parities) and a continuum in which the  $I\Pi$  independent component  $\rho_T^{I\Pi}(E)$  is continuously adjusted to the higher discrete excited states as explained above for the  $CN$  level density (fig. 1-9). The discrete level schemes which are adopted are given in Tables 3-10. The adjusted parameters {  $E_x$ ,  $E_0$ ,  $T$  } and the level density parameters "a" obtained for each nucleus are shown in Table 11. These level density parameters "a" are calculated using the average s-wave level spacing  $\langle D \rangle$  determined from resolved resonance parameter measurements [12,13,16,19], the neutron binding energy  $B_n$  [20], and the Cook's values [21] for the pairing energy  $\delta$ . The experimental and adopted values of  $\langle D \rangle$  are given in Tables 1-2.

. Below  $E_n = 3$  MeV, the Weisskopf formula [22] is adopted for the energy variation of  $\Gamma_{\gamma}^{JII}$ . For excitation energies close to  $B_n$ , the average widths  $\langle \Gamma_{\gamma} \rangle_{exp}$  are determined from s-wave resolved resonances ; the width  $\Gamma_{\gamma}(E)$  is then normalized to  $\langle \Gamma_{\gamma} \rangle_{exp}$  at  $E = B_n$ . The experimental [23,24,25] and adopted values of  $\langle \Gamma_{\gamma} \rangle$  are given in Tables 1-2. Except for the ( $n + {}^{148}Sm$ ) compound system for which no  $\langle \Gamma_{\gamma} \rangle$  measurements are available, the adopted values for  $\langle D \rangle$  and  $\langle \Gamma_{\gamma} \rangle$  are within the experimental uncertainties.

The present results of capture cross section calculations using the statistical model code NCNR [26] are shown in fig. 10-16 for the even and odd samarium isotopes. It is generally difficult to claim a good agreement between calculations and measurements [27,28] which are rather scarce except for  ${}^{154}Sm$ . For this target nucleus, the present calculations are in good agreement with the Fawcett measurements [27] below 150 keV.

The structure effects of the  ${}^{150}Sm$  target nucleus on the calculated capture cross section is shown in fig. 17. This effect is small in the energy range below 3 MeV.

In fig. 10-16 are shown the previous calculations by Benzi et al. [29], RIBON et al. [13] and the ENDF/B IV evaluations.

#### IV - DISCUSSION -

When all these calculations are compared, it is possible to do some remarks :

a)  ${}^{147}Sm$  (fig. 10).

The capture cross sections values show a very large dispersion in the full energy range and especially above 1 MeV. This is in part due to the various choice of density laws in the continuum for the target and the compound nucleus.

b)  ${}^{148}Sm$  (fig. 11).

Up to 40 keV neutron-energy, there is a qualitative agreement between the calculated values. Above a few hundred keV, the dispersions of the curves have roughly the same magnitudes as previously observed for  ${}^{147}Sm$ .

c)  $^{149}\text{Sm}$  (fig. 12).

The present calculation is in close agreement with the one by Ribon et al. [13] up to about 40 keV energy. There is a good agreement between the four curves between 10 keV and 300 keV.

d)  $^{150}\text{Sm}$  (fig. 13) and  $^{152}\text{Sm}$  (fig. 15).

Below 300 keV neutron energy, the same comment as in c) can be made.

e)  $^{154}\text{Sm}$  (fig. 16).

The calculated cross sections have strengths which show a large dispersion in the full energy range. The present work is however in qualitative agreement with the ENDF/B IV evaluation.

f)  $^{151}\text{Sm}$  (fig. 14).

In the calculations by Ribon et al. [13], many excited states have been added to the experimental level sequence. These supplementary states have been excluded from the present work, the result of which is shown in fig. 14 and compared to the one by Ribon et al. The new calculations -this work- which are presented have been performed using the Kirouac et al. [12] measurements for  $\langle\Gamma_\gamma\rangle$  and  $\langle D \rangle$  level parameters (cf. Table 2). The strength and energy variation of the present calculated capture cross sections are not strongly different from the Ribon et al. one's.

In conclusion, the above results obtained for the exemple of the samarium isotopes, show that an overall coherence seems to be obtainable by using an unified parameterization of the optical potential within the full energy range of interest. Moreover, this procedure permits us to extrapolate with more confidence to the case of unstable targets.

REFERENCES

- [1] - GRUPPELAAR, H., *Nuclear Theory in neutron nuclear data evaluation*, IAEA-190 (1976).
- [2] - DELAROCHE, J.P., LAGRANGE, Ch., SALVY, J., *Nuclear theory in neutron nuclear data evaluation*, IAEA-190 (1976).
- [3] - LAGRANGE, Ch., *Proc. Nat. Soviet Conf. on neutron physics*, KIEV (1975), *Neutronaia Fysika* (1976).
- [4] - LAGRANGE, Ch., SHAMU, R.E., BURROWS, T., GLASGOW, G.P., HARDIE, G., McDANIEL, F.D., *Phys. Lett.* 58B 3 (1975) 293.  
SHAMU, R.E., LAGRANGE, Ch., BERNSTEIN, E.M., RAMIREZ, J.J., TAMURA, T., WONG, C.Y., *Phys. Lett.* 61B 1 (1976) 29.  
McELLISTREM, M.T., SHAMU, R.E., LACHKAR, J., HAOUAT, G., LAGRANGE, Ch., PATIN, Y., SIGAUD, J., COÇU, F., *Phys. Rev. C15* 3 (1977) 927.
- [5] - SHAMU, R.E., HAOUAT, G., LACHKAR, J., McELLISTREM, M.T., LAGRANGE, Ch., SIGAUD, J., DELAROCHE, J.P., PATIN, Y., COÇU, F., *Proc. Int. Conf. on the Interact. of neutrons with Nuclei*, LOWELL (1976), CONF-760715-P2, p. 1327.
- [6] - TAMURA, T., *ORNL-4152*.
- [7] - EILAND, H.M., WEINSTEIN, S., SEEMAN, K.W., *BNL-50298* (1971) 172.
- [8] - KARZHAVINA, E.N., POPOV, A.B., *Sov. Nucl. Phys.* 15 (1972) 225.
- [9] - MUSGROVE, A.R. de L., *AAEC/E277* (1973).

- [10] - SETH, K.K., *Nucl. Data* 2 (1966) 299.
- [11] - CAMARDA, H., LIOU, H.I., RAHN, F., HACKEN, G., SLAGOWITZ, M., HAVENS, W.W. JR., RAINWATER, J., WYNCHANK, S., *Proc. ALBANY Conf.* (1972).
- [12] - KIROUAC, G.J., EILAND, H.M., *Phys. Rev.* C11 3 (1975) 895.
- [13] - RIBON, P., FORT, E., KREBS, J., QUOC THUANG, T., *CEA-N-1832* (1975).
- [14] - EILAND, H.M., WEINSTEIN, S., SEEMANN, K.W., *Nucl. Sc. Eng.* 54 (1974) 286.
- [15] - RAHN, F., CAMARDA, H.S., HACKEN, G., HAVENS, W.W. JR., LIOU, H.I., RAINWATER, J., SLAGOWITZ, M., WYNCHANK, S., *Phys. Rev.* C6 (1972) 251.
- [16] - BNL-325, Third Edition (1973).
- [17] - MOLDAUER, P.A., *Phys. Rev.* 135B (1964) 642 ; *Rev. Mod. Phys.* 36 (1964) 1079.
- [18] - GILBERT, A., CAMERON, A.G.W., *Can. J. Phys.* 43 (1965) 1446.
- [19] - SOLOVIEV, V.G., STOYANOV, Ch., VDOVIN, A.I., *Nucl. Phys.* A224 (1974) 411.
- [20] - WAPSTRA, A.H., GOVE, N.B., *Nucl. Data Tables*, 9 N° 4-5 (1971).
- [21] - COOK, J.L., FERGUSON, H., MUSGROVE, A.R. de L., *Aust. J. Phys.* 20 (1967) 477.
- [22] - BLATT, J.M., WEISSKOPF, V.F., *Theoretical Nuclear Physics* (John Wiley and Sons, Inc.) N.Y. (1952).
- [23] - GOULASSY, M., PERKINS, S.T., *UCRL-50400*, Vol. 13.
- [24] - BECVAR, F., CHRIEN, R.E., WASSON, O.A., *Nucl. Phys.* A236 (1974) 198.
- [25] - RAHN, F., CAMARDA, H.S., HACKEN, G., HAVENS, W.W. JR., LIOU, H.I., RAINWATER, J., SLAGOWITZ, M., WYNCHANK, S., *Nucl. Sc. Eng.* 48 (1972) 219.

- [26] - THOMET, P., *unpublished*.
- [27] - FAWCETT, L.R., KEITH FURR, A., LINDSAY, J.G., *Nucl. Sc. Eng.*, 49 (1972) 317.
- [28] - MACKLIN, R.L., GIBBONS, J.H., INADA, T., *Nature* 197 (1963) 369.
- JOHNSRUD, A.E., SILBERT, M.G., BARSCHALL, H.H., *Phys. Rev.* 116 (1959) 927.
- MACKLIN, R.L., LAZAR, N.H., LYON, W.S., *Phys. Rev.* 107 (1957) 504.
- CHAUBEY, A.K., SEHGAL, M.L., *Phys. Rev.* 152 (1966) 1055.
- PETO, G., MILIGY, Z., HUNYADI, I., *J. Nucl. Energ.* 21 (1967) 797.
- LYON, W.S., MACKLIN, R.L., *Phys. Rev.* 114 (1959) 1619.
- [29] - BENZI, V., ORAZI, R.d', REFFO, G., VACCARI, M., *CEC* (71) 9.
- [30] - Nuclear Data Sheets 10 (1973) 429.
- [31] - Nuclear Data Sheets 15 (1975) 4.
- [32] - GARRETT, C., LEIGH, J.R., DRACOULIS, G.D., *Nucl. Phys.* A262 (1976) 137.
- [33] - Nuclear Level Schemes, A = 45 through A = 257, from Nuclear Data Sheets, ACADEMIC PRESS, INC. (1973).
- [34] - OELERT, W., MAHER, J.V., SINK, D.A., SPISAK, M.J., *Phys. Rev.* C12 (1975) 417.
- [35] - OELERT, W., LINDSTRÖM, G., RIECH, V., *Nucl. Phys.* A233 (1974) 237.
- [36] - VEJE, E., ELBECK, B., HERSKIND, B., OLESEN, M.C., *Nucl. Phys.* A109 (1968) 489.

- [37] - BOHR, A., MOTTELSON, B.R., *Nuclear Structure*, Vol. 2, p. 534 and 577,  
W.A. BENJAMIN, INC. (1975).
- [38] - BJERREGAARD, J.H., HANSEN, O., NATHAN, O., *Nucl. Phys.* 86 (1966) 145.
- [39] - BECVAR, F., CHRIEN, R.E., WASSON, O.A., *Nucl. Phys.* A236 (1974) 173.
- [40] - OELERT, W., MAHER, J.V., SINK, D.A., SPISAK, M.J., *Phys. Rev.* C12  
(1975) 1495.
- [41] - COOK, W.B., JOHNS, M.W., LOVHOIDEN, G., WADDINGTON, J.C., *Nucl. Phys.*  
A259 (1976) 461.
- [42] - WIRTH, G., KAFFRELL, N., CHAYAWATTANANGKUR, K., HERRMANN, G., SEYB, K.E.,  
*Z. Phys.* A272 (1975) 291.
- [43] - EJIRI, H., SHIBATA, T., SHIMIZU, A., YAGLI, K., *Jour. Phys. Soc. Japan*,  
33 (1972) 1515.
- [44] - D'AURIA, J.M., OSTROM, D., GUJRATHI, S.C., *Nucl. Phys.* A178 (1971) 172.
- [45] - ELBAKR, S.A., VAN HEERDEN, I.J., ROBERTSON, B.C., McDONALD, W.J.,  
NEILSON, G.C., DAWSON, W.K., *Nucl. Phys.* A211 (1973) 493.

Samarium isotopes. Compound system averaged parameters

Target	$^{147}\text{Sm}$	$^{148}\text{Sm}$	$^{149}\text{Sm}$	$^{150}\text{Sm}$
$^{10^4} \text{S}_0$ (exp.)	4.60±0.40 (1) 3.70±0.80 (2) 4.35±0.50 (3)		3.00±1.00 (4) 5.10±0.90 (2) 4.50±1.00 (3) 5.20 (7)	3.60±0.30 (1) 3.60±0.30 (3) 3.30±1.10 (8)
$^{10^4} \text{S}_0$ (calc.)	3.62 (9)	3.62 (9)	4.62 (9)	5.58(Vibr.) (9) 5.65(Rot.) (9) 5.62 (9)
$^{10^4} \text{S}_1$ (exp.)			0.60 (7)	
$^{10^4} \text{S}_1$ (calc.)	1.28 (9)	1.28 (9)	1.34 (9)	1.84(Vibr.) (9) 1.30(Rot.) (9) 1.40 (9)
$\langle D \rangle$ (eV) (exp.)	7.40±0.70 (11)	90±15 (12)	2.30±0.30 (11) 2.05±0.17 (7)	68±10 (11)
$\langle D \rangle$ (eV) ADOPTED	7.40 (9)	75 (9)	2.10 (9)	60 (9)
$\langle \Gamma_Y \rangle$ (meV) (exp.)	71±27 (13)		61.50±1.50 (7)	64.6 (14)
$\langle \Gamma_Y \rangle$ (meV) ADOPTED	95 (9)	50 (9)	62 (9)	60 (9)

- |          |      |                  |      |
|----------|------|------------------|------|
| (1) Ref. | [7]  | (8) Ref.         | [14] |
| (2) Ref. | [8]  | (9) Present work |      |
| (3) Ref. | [9]  | (10) Ref.        | [15] |
| (4) Ref. | [10] | (11) Ref.        | [16] |
| (5) Ref. | [11] | (12) Ref.        | [19] |
| (6) Ref. | [12] | (13) Ref.        | [23] |
| (7) Ref. | [13] | (14) Ref.        | [24] |

TABLE 1

Samarium Isotopes. Compound system averaged parameters

Target	$^{151}\text{Sm}$	$^{152}\text{Sm}$	$^{154}\text{Sm}$
$^{10^4}\text{S}_0$ (exp.)	$3.50 \pm 1.90$ (4) $3.65 \pm 0.48$ (6) 3.50 (7)	$2.72 \pm 0.83$ (5) $2.70 \pm 0.80$ (3) $2.20 \pm 0.40$ (10) $2.20 \pm 0.40$ (11)	$1.90 \pm 0.66$ (5) $1.90 \pm 0.70$ (3) $1.80 \pm 0.50$ (10) $1.80 \pm 0.50$ (11)
$^{10^4}\text{S}_0$ (calc.)	3.81 (9)	2.00 (9)	1.37 (9)
$^{10^4}\text{S}_1$ (exp.)	0.80 (7)		
$^{10^4}\text{S}_1$ (calc.)	1.40 (9)	1.39 (9)	1.45 (9)
$\langle D \rangle$ (eV) (exp.)	$0.90 \pm 0.18$ (7) $1.72 \pm 0.12$ (6)	$51.80 \pm 4.30$ (11)	$115 \pm 14$ (11)
$\langle D \rangle$ (eV) ADOPTED	1.72 (9)	50 (9)	115.80 (9)
$\langle \Gamma_\gamma \rangle$ (meV) (exp.)	$75 \pm 5$ (7) 98 (6)	$65 \pm 13$ (15)	$79 \pm 16$ (15)
$\langle \Gamma_\gamma \rangle$ (meV) ADOPTED	98 (9)	65 (9)	80 (9)

- (3) Ref. [9]
- (4) Ref. [10]
- (5) Ref. [11]
- (6) Ref. [12]
- (7) Ref. [13]
- (8) Ref. [14]
- (9) Present work

- (10) Ref. [15]
- (11) Ref. [16]
- (12) Ref. [19]
- (13) Ref. [23]
- (14) Ref. [24]
- (15) Ref. [25]

TABLE 2

$^{147}_{\text{Sm}}$ 

## Adopted level scheme

$E^*(\text{MeV})$	$I \pi$
0.000	$7/2^-$
0.121	$5/2^-$
0.197	$3/2^-$
0.716	$11/2^-$
0.799	$3/2^-$
0.808	$9/2^-$
0.925	$5/2^-$
1.007	$1/2^-$
1.029	$3/2^-$
1.054	$5/2^+$
1.065	$5/2^+$
1.077	$7/2^-$

Ref. [32,33]

TABLE 3

$^{148}_{\text{Sm}}$

Adopted level scheme

E* (MeV)	I π
0.000	0 +
0.550	2 +
1.120	0 +
1.161	3 -
1.180	4 +
1.380	0 +
1.427	0 +
1.434	1 -
1.453	2 +
1.465	1 -
1.594	5 -
1.649	2 +
1.663	2 +
1.733	4 +

Ref. [34,35,36,37]

TABLE 4

$^{149}_{\text{Sm}}$

Adopted level scheme

$E^*(\text{MeV})$	$I \pi$
0.000	7/2 -
0.022	5/2 -
0.277	7/2 -
0.286	3/2 -
0.350	3/2 -
0.393	1/2 -
0.528	3/2 -
0.558	5/2 -
0.590	9/2 -
0.606	3/2 -
0.636	7/2 -
0.649	3/2 +
0.660	11/2 -
0.677	5/2 -
0.695	1/2 -
0.709	3/2 -
0.722	5/2 +
0.760	3/2 -
0.785	5/2 -
0.814	7/2 +
0.820	9/2 -
0.830	5/2 +
0.833	1/2 +
0.860	1/2 -
0.870	3/2 -

Ref. [13,32]

TABLE 5

$^{152}_{\text{Sm}}$ 

## Adopted level scheme

$E^*$ (MeV)	$I \pi$
0.000	0 +
0.122	2 +
0.366	4 +
0.685	0 +
0.712	6 +
0.811	2 +
0.939	1 +
0.963	1 -
0.988	2 +
1.026	4 +
1.042	3 -
1.083	0 +
1.087	2 +
1.091	0 +
1.125	8 +

Ref. [35,36,37,38,42,43]

TABLE 6

$^{150}_{\text{Sm}}$ 

Adopted level scheme

$E^*(\text{MeV})$	$I \pi$
0.000	0 +
0.334	2 +
0.737	2 +
0.740	0 +
0.773	4 +
1.045	2 +
1.071	3 -
1.083	2 -
1.165	2 +
1.193	2 +
1.196	1 -
1.256	0 +
1.279	6 +

Ref. [24,35,36,38,39,40]

TABLE 7

$^{151}_{\text{Sm}}$

Adopted level scheme

$E^*$ (MeV)	I $\pi$
0.000	5/2 -
0.005	3/2 -
0.066	7/2 -
0.070	5/2 -
0.092	9/2 +
0.105	3/2 -
0.148	13/2 +
0.1677	5/2 +
0.1684	5/2 -
0.175	9/2 -
0.209	7/2 -
0.246	7/2 +
0.261	11/2 -
0.284	1/2 -
0.295	9/2 -
0.303	5/2 -
0.307	3/2 +
0.313	1/2 +
0.315	3/2 -
0.324	7/2 +
0.345	3/2 +
0.357	1/2 +
0.383	17/2 +
0.395	5/2 +
0.396	5/2 +
0.405	7/2 -
0.416	5/2 -
0.424	11/2 -
0.445	13/2 -
0.446	5/2 +

Ref. [13,41]

TABLE 8

$^{154}_{\text{Sm}}$

Adopted level scheme

$E^*$ (MeV)	I $\pi$
0.000	0 +
0.082	2 +
0.267	4 +
0.547	6 +
0.906	8 +
0.922	1 -
0.927	8 +
1.012	3 -
1.100	0 +
1.120	2 +
1.178	2 +
1.181	5 -
1.202	0 +
1.220	0 +
1.286	3 -

Ref. [36,38,44,45]

TABLE 9

$^{153}_{\text{Sm}}, ^{155}_{\text{Sm}}$

ADOPTED LEVEL SCHEME : Ref [30,31]

TABLE 10

Samarium isotopes. Level density parameter values

Density at  
low excitation energy       $(E^* \leq E_x)$        $\rho_1(E^*) \sim \exp \left[ (E^* - E_0)/T \right]$

Density at  
high excitation energy       $(E^* \geq E_x)$        $\rho_2(E^*) \sim \exp \left[ 2\sqrt{a(E^* - \delta)} \right]$

Nucleus	$E_0$ (MeV)	T (MeV)	$B_n$ (MeV)	$\delta$ (MeV)	$a$ (MeV $^{-1}$ )	$E_x$ (MeV)
$^{147}\text{Sm}$	- 0.250	0.534	6.373	0.980	18.539	4.479
$^{148}\text{Sm}$	0.200	0.582	8.141	2.090	19.069	6.644
$^{149}\text{Sm}$	- 0.800	0.519	5.873	0.980	21.836	5.166
$^{150}\text{Sm}$	- 0.100	0.5435	7.986	1.930	21.574	6.528
$^{151}\text{Sm}$	- 1.360	0.532	5.596	0.810	22.839	5.545
$^{152}\text{Sm}$	- 0.400	0.567	8.266	1.910	21.396	6.956
$^{153}\text{Sm}$	- 1.300	0.539	5.867	0.850	22.348	5.589
$^{154}\text{Sm}$	- 0.300	0.581	7.978	2.110	21.061	7.332
$^{155}\text{Sm}$	- 0.860	0.535	5.814	0.830	20.580	4.966

TABLE 11

FIGURE CAPTIONS

FIGURE 1 : Cumulated level diagram for  $^{147}\text{Sm}$ . Comparison between experimental and adjusted theoretical values.

FIGURE 2 : Cumulated level diagram for  $^{148}\text{Sm}$ . Comparison between experimental and adjusted theoretical values.

FIGURE 3 : Cumulated level diagram for  $^{149}\text{Sm}$ . Comparison between experimental and adjusted theoretical values.

FIGURE 4 : Cumulated level diagram for  $^{150}\text{Sm}$ . Comparison between experimental and adjusted theoretical values.

FIGURE 5 : Cumulated level diagram for  $^{151}\text{Sm}$ . Comparison between experimental and adjusted theoretical values.

FIGURE 6 : Cumulated level diagram for  $^{152}\text{Sm}$ . Comparison between experimental and adjusted theoretical values.

FIGURE 7 : Cumulated level diagram for  $^{153}\text{Sm}$ . Comparison between experimental and adjusted theoretical values.

FIGURE 8 : Cumulated level diagram for  $^{154}\text{Sm}$ . Comparison between experimental and adjusted theoretical values.

FIGURE 9 : Cumulated level diagram for  $^{155}\text{Sm}$ . Comparison between experimental and adjusted theoretical values.

FIGURE 10 : Measured and calculated capture cross section for  $^{147}\text{Sm}$ .

FIGURE 11 : Measured and calculated capture cross section for  $^{148}\text{Sm}$ .

FIGURE 12 : Measured and calculated capture cross section for  $^{149}\text{Sm}$ .

FIGURE 13 : Measured and calculated capture cross section for  $^{150}\text{Sm}$ .

FIGURE 14 : Measured and calculated capture cross section for  $^{151}\text{Sm}$ .

FIGURE 15 : Measured and calculated capture cross section for  $^{152}\text{Sm}$ .

FIGURE 16 : Measured and calculated capture cross section for  $^{154}\text{Sm}$ .

FIGURE 17 : Calculated capture cross section for  $^{150}\text{Sm}$  assuming the vibrational  
and rotational models.

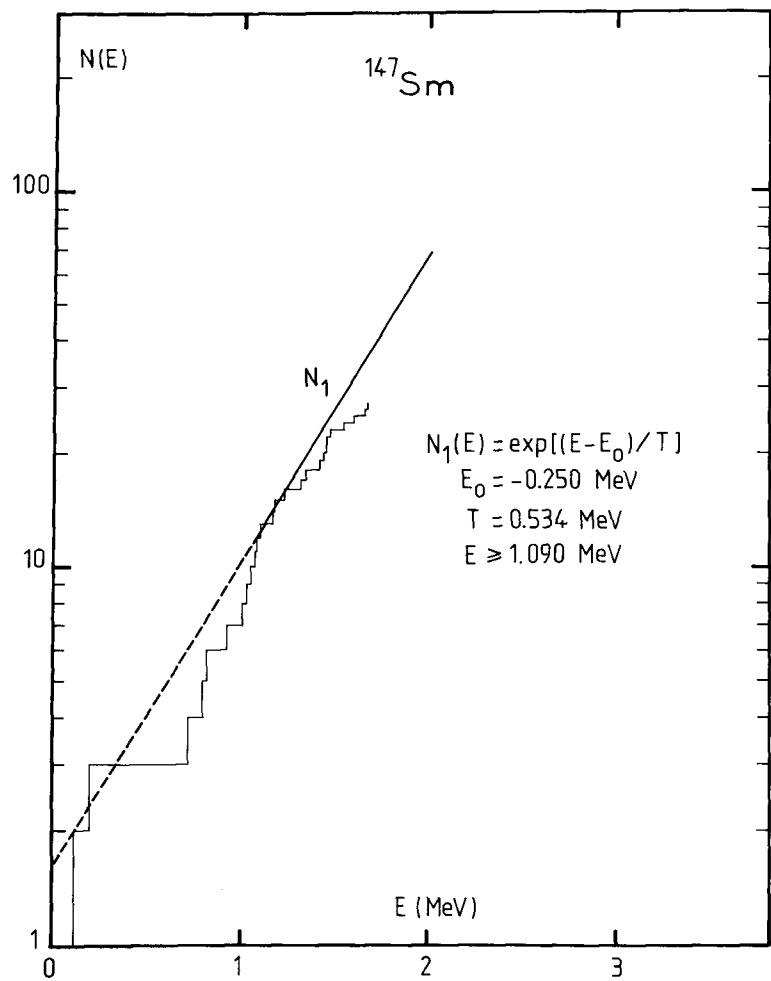


FIG. 1

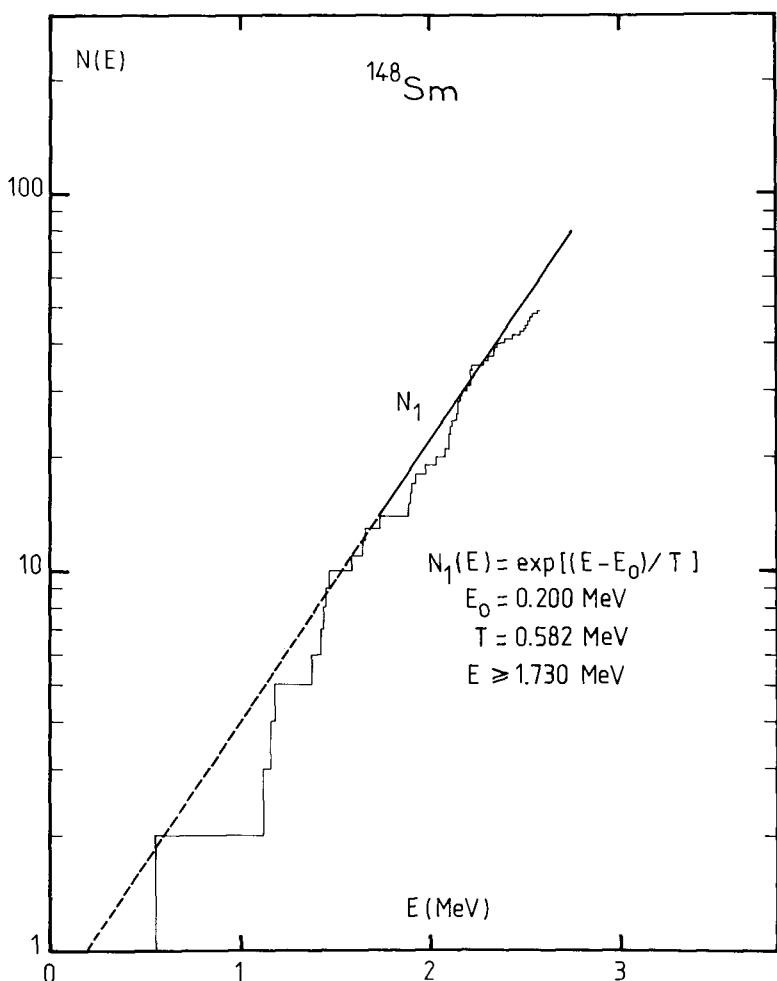


FIG. 2

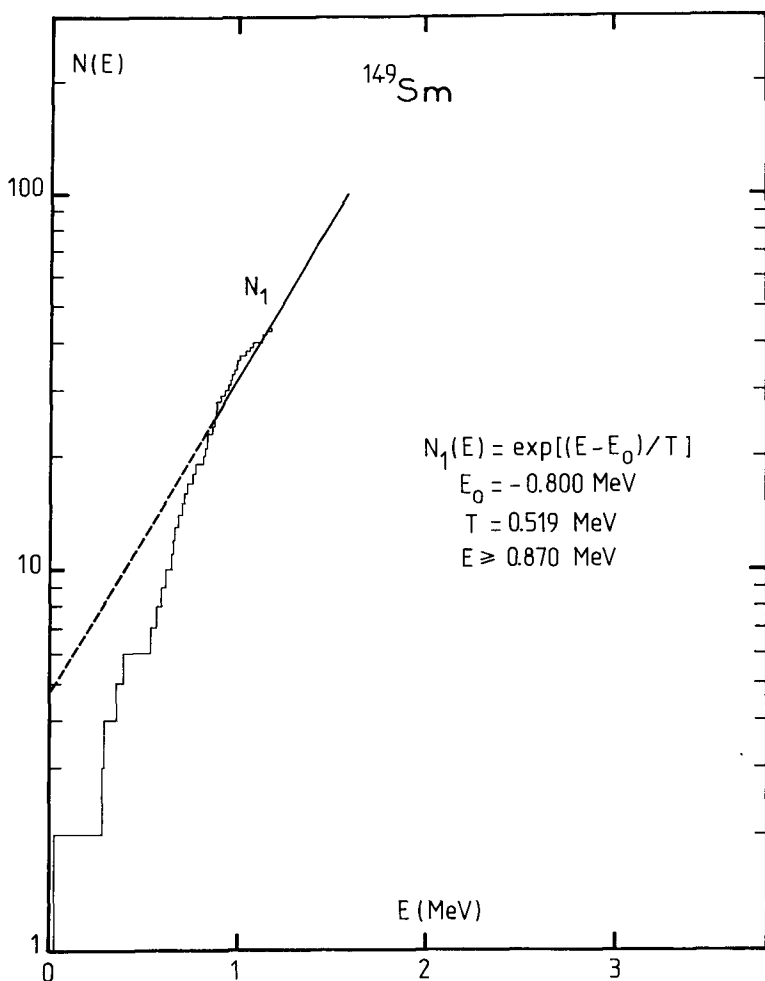


FIG. 3

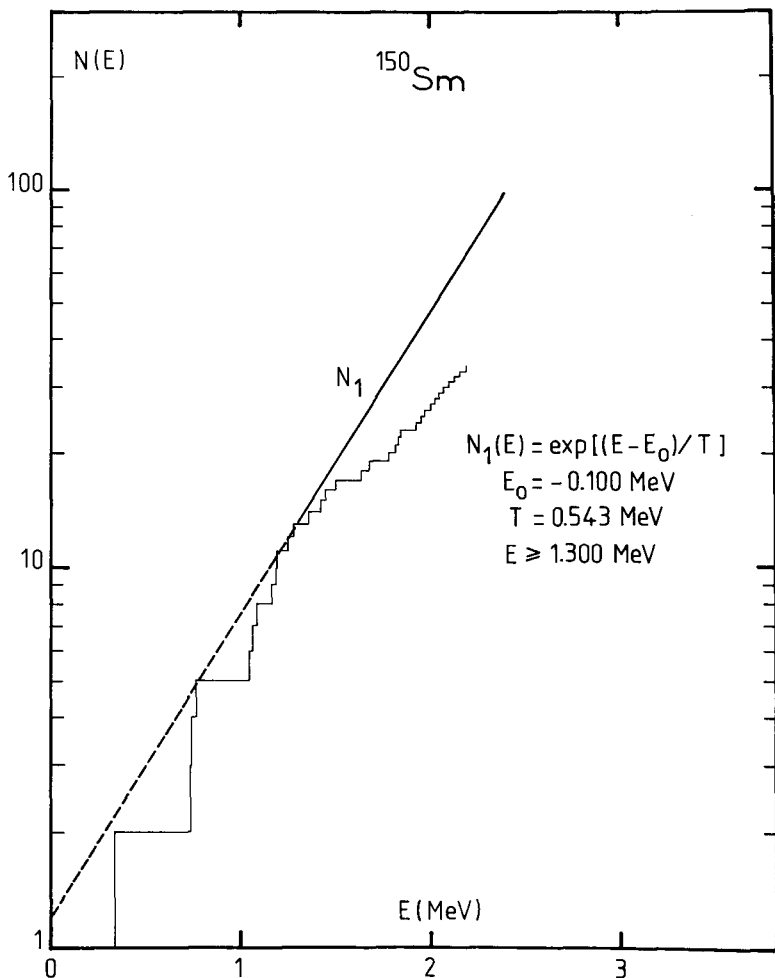


FIG. 4

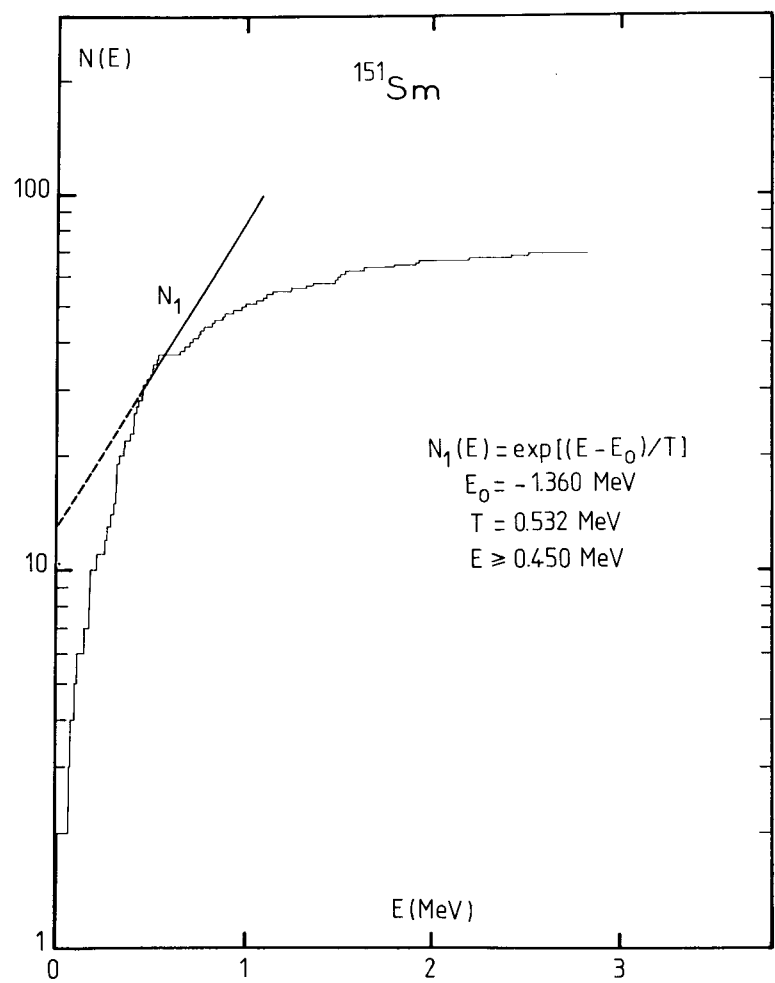


FIG. 5

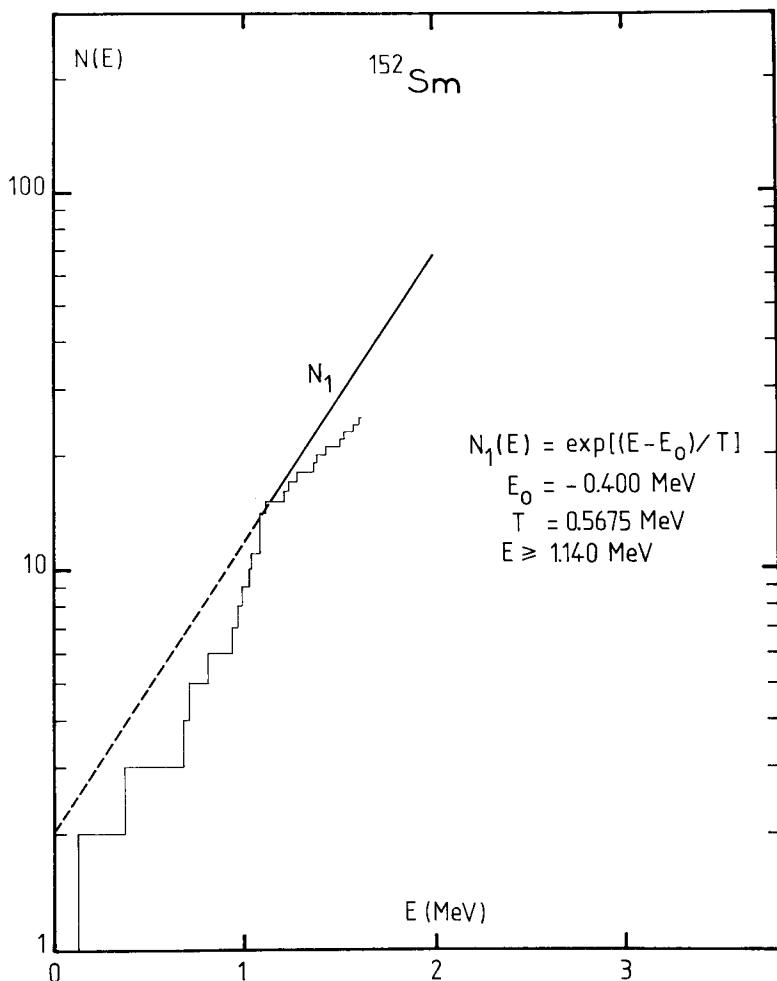


FIG. 6

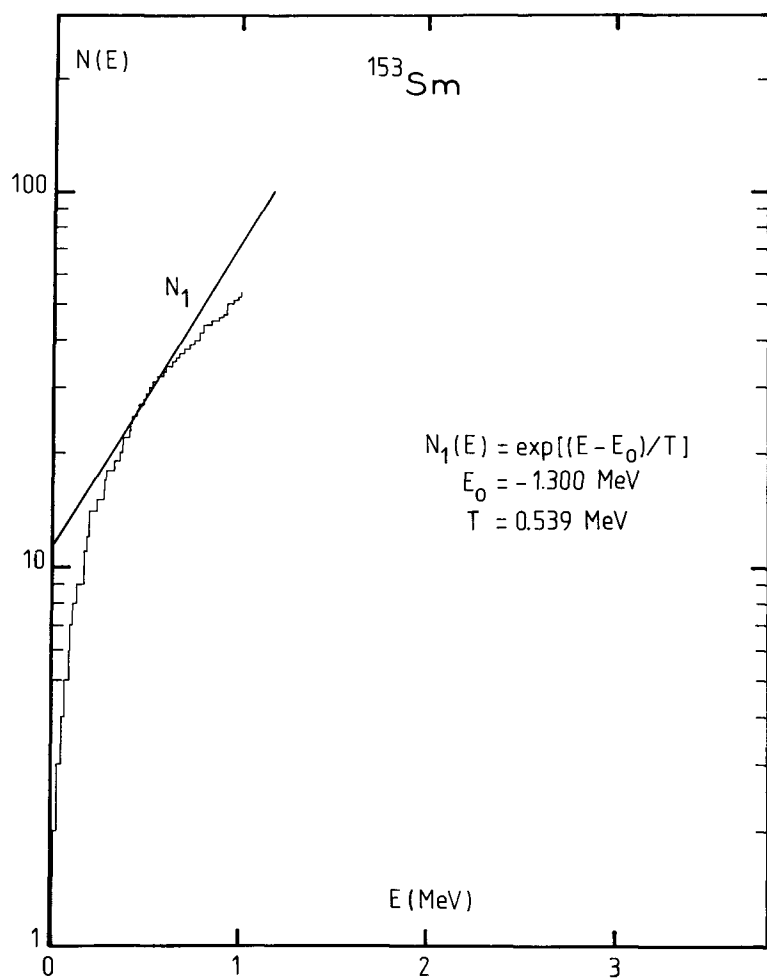


FIG. 7

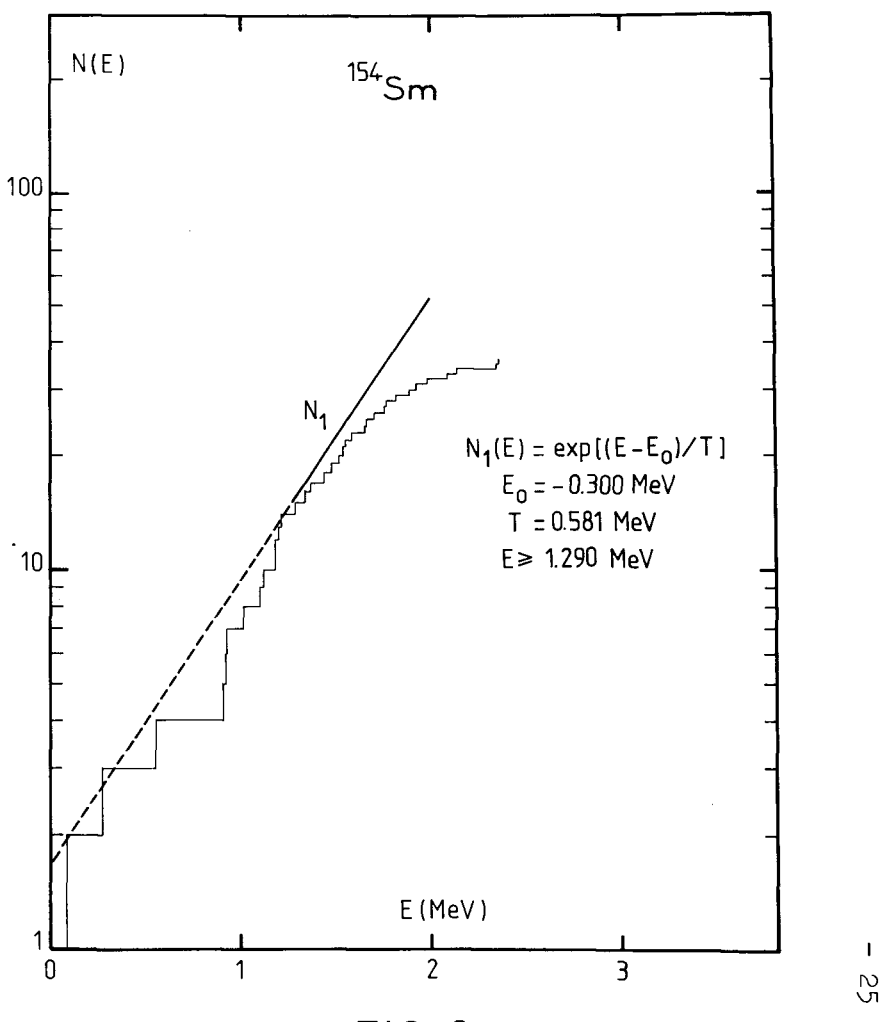


FIG. 8

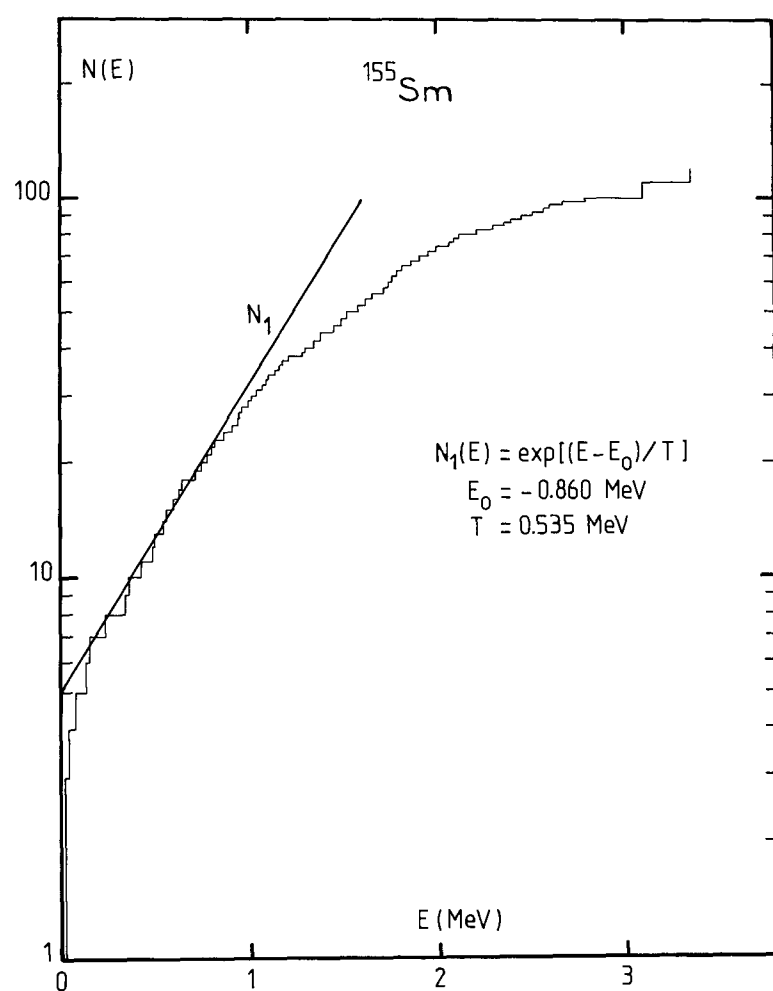


FIG. 9

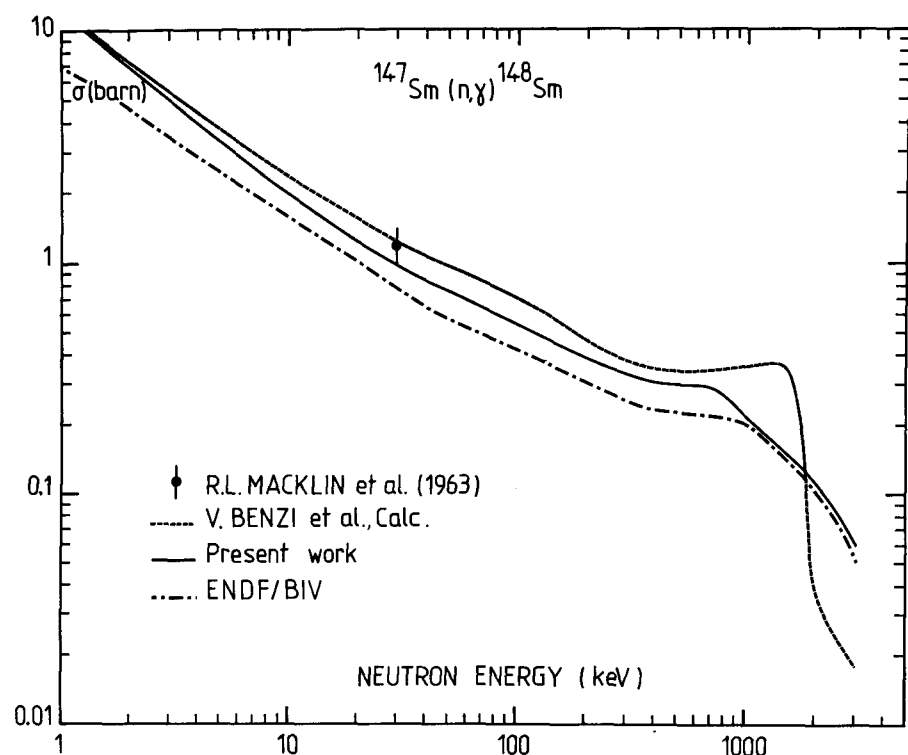


FIG. 10

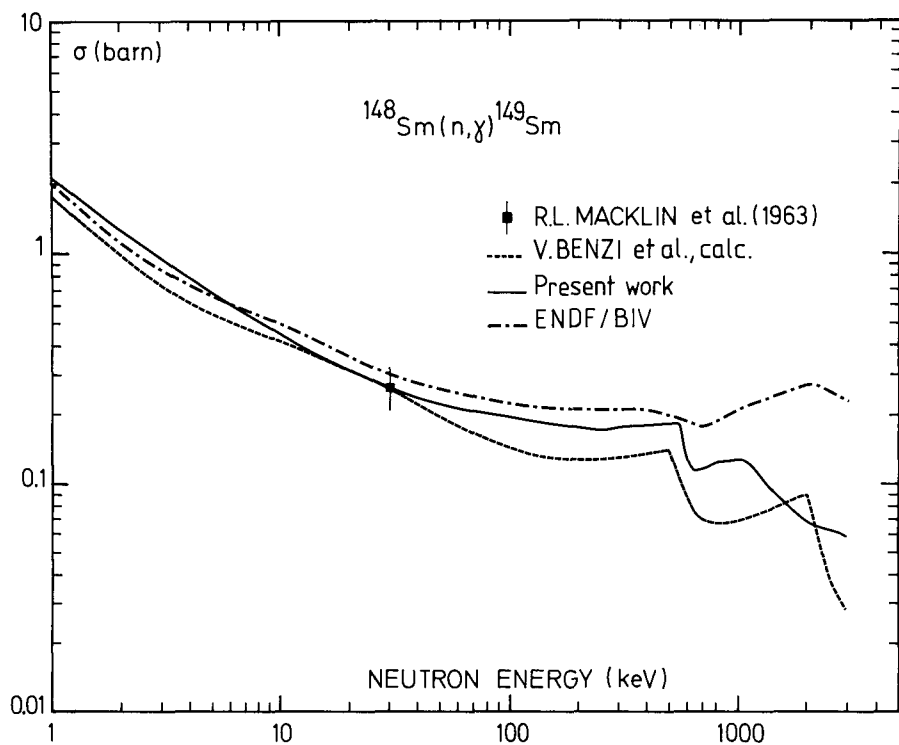


FIG.11

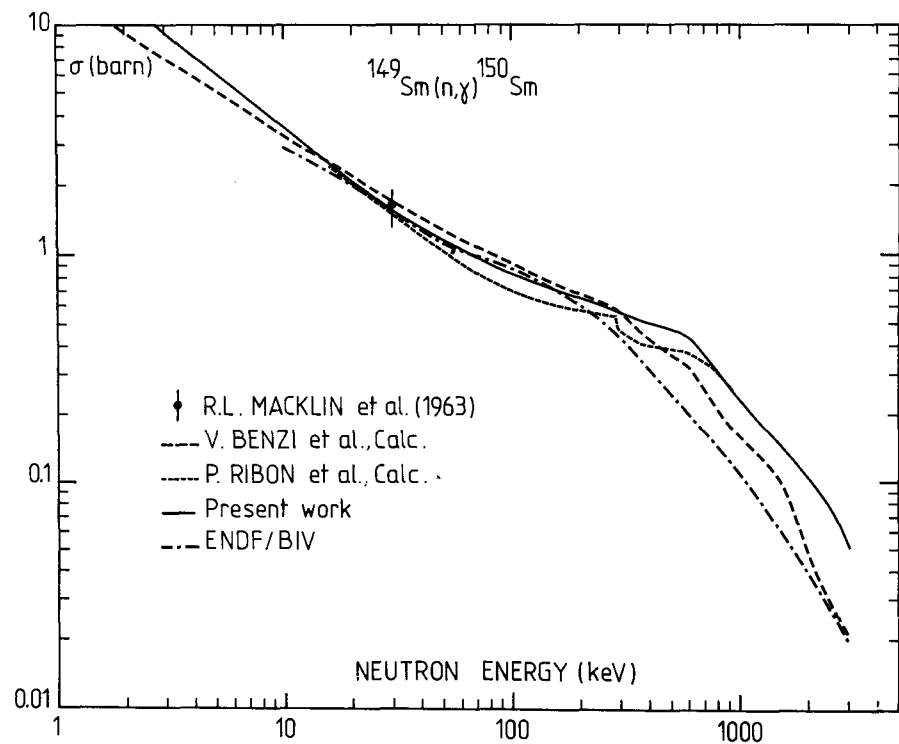


FIG.12

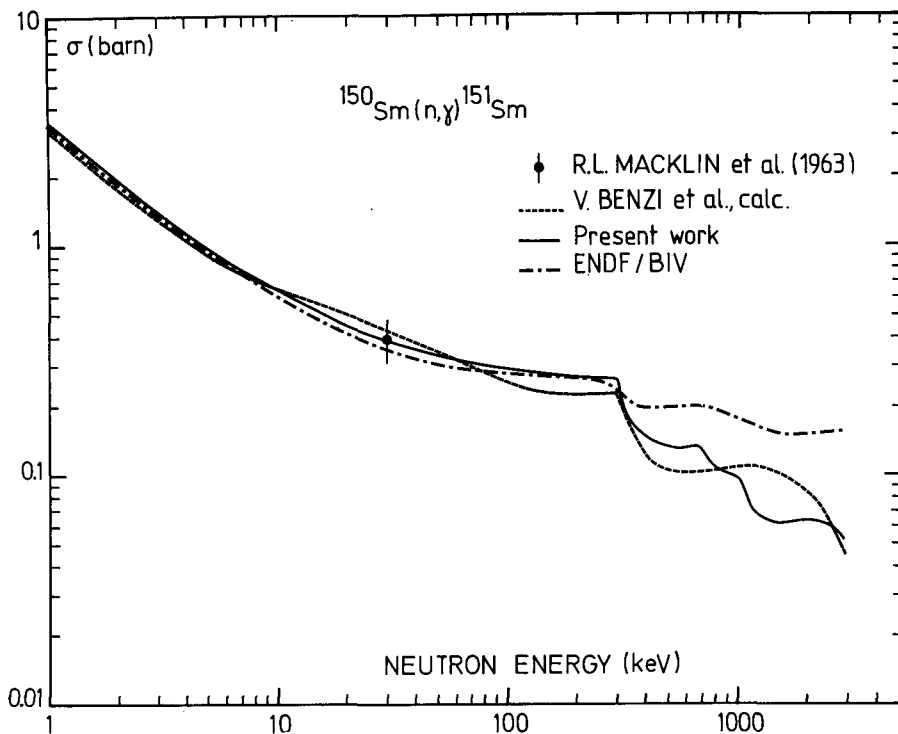


FIG. 13

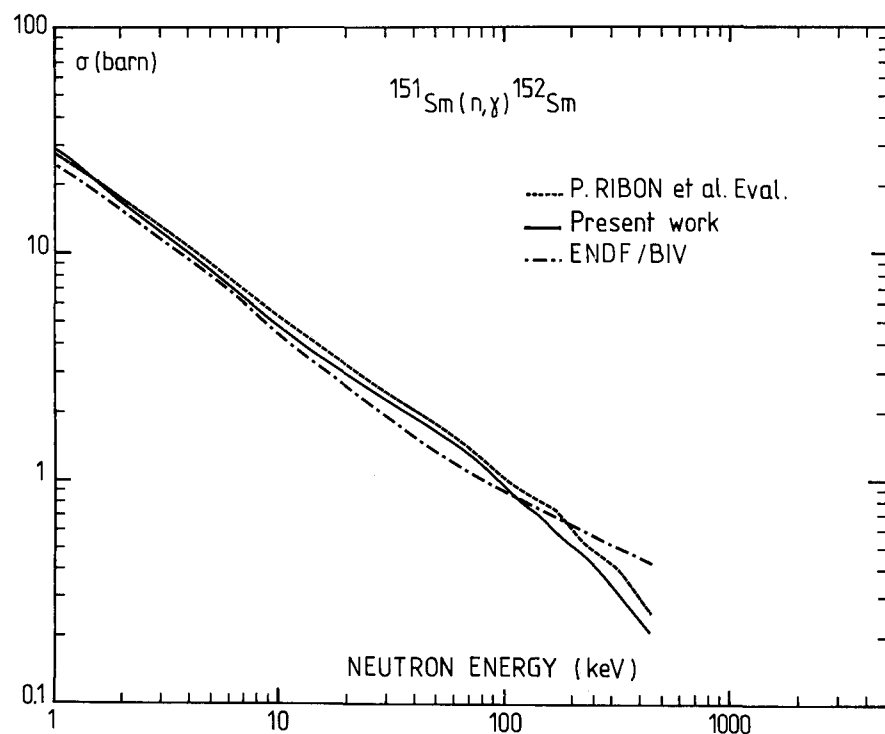


FIG. 14

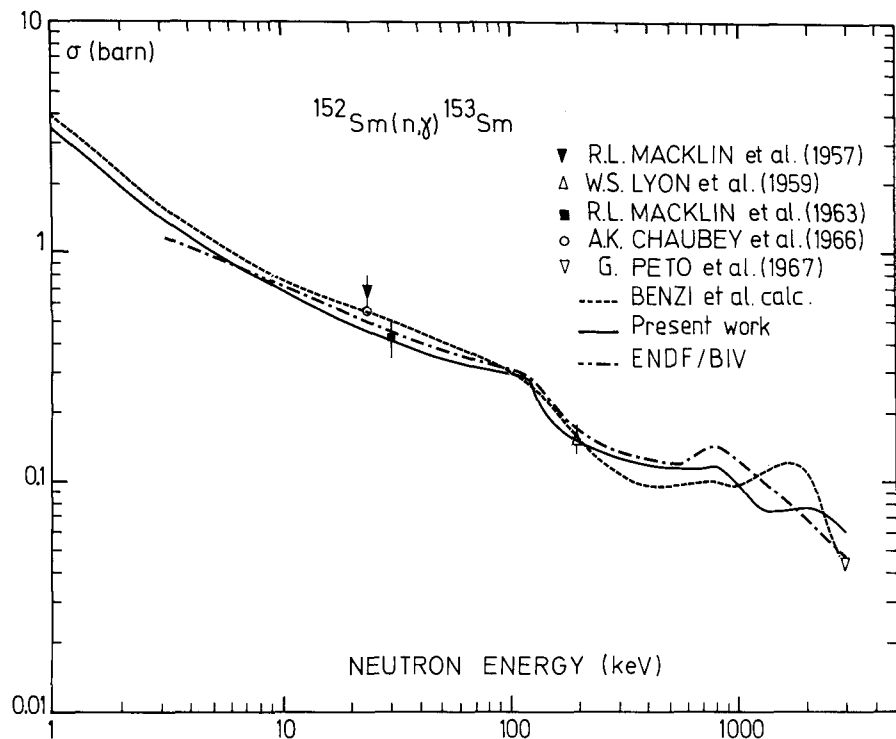


FIG.15

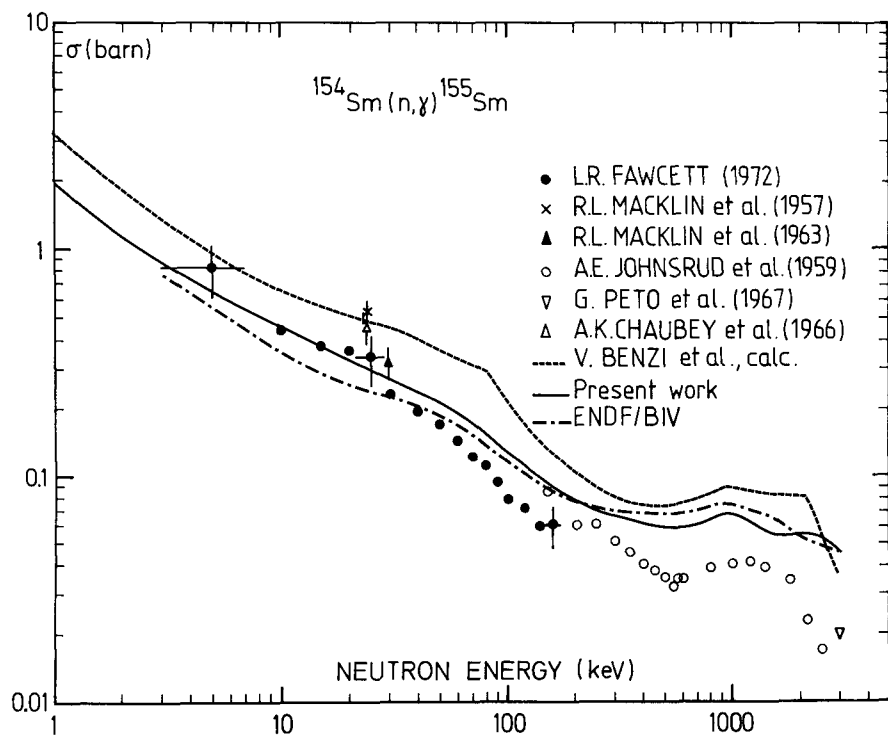


FIG.16

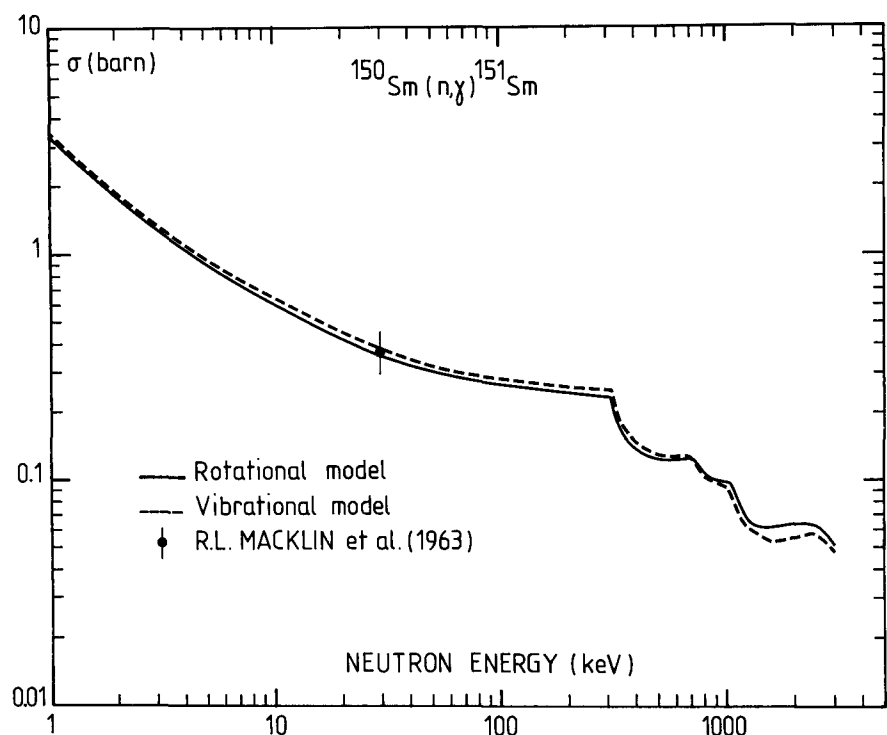


FIG. 17